View Article Online / Journal Homepage / Table of Contents for this issue
Dynamic Article Links

Polymer Chemistry

Cite this: *Polym. Chem.*, 2012, **3**, 1033

www.rsc.org/polymers

PAPER

An improved grafting technique for producing imprinted thin film composite beads†

Mahadeo R. Halhalli, Carla S. A. Aureliano, Eric Schillinger, Claudia Sulitzky, M. Magdalena Titirici‡ and Börje Sellergren*

Received 14th November 2011, Accepted 30th December 2011
DOI: 10.1039/c2py00544a

Published on 06 February 2012. Downloaded by Michigan State University on 27/01/2016 02:24:16.

Thin molecularly imprinted polymer (MIP) films were grafted from porous silica using immobilized azoinitiators in the absence or presence of RAFT mediated control or by controlled radical polymerization using immobilized iniferters. The resulting composites were compared in terms of film thickness, the grafted layer homogeneity, effect of different support morphologies and their chromatographic performance regarding enantioselectivity, and efficiency. Film thickness was controlled either kinetically by interrupted polymerization or stoichiometrically based on complete monomer conversion. Thus, L-phenylalanine anilide (L-PA) imprinted poly(MAA-*co*-EDMA) silica composites prepared by the former technique using the iniferter modified supports exhibited heterogeneous distribution of grafted polymer as shown by the absence of correlations between the pore system parameters and the graft density. This contrasted with the linear correlations observed by both the kinetic and stoichiometric grafting techniques based on azoinitiator or RAFT modified supports indicating that these exhibit homogeneous grafted films. These results were corroborated by chromatographic tests. Whereas the iniferter composites produced by interrupted polymerization were not capable of racemic resolution and generally showed very low or non-existent enantioselectivity, the azo-composites showed a pronounced enantioselectivity which was strongly dependent on the film thickness, monomer dilution, the RAFT/initiator ratio and the method of grafting. Hence, composites prepared by exhaustive polymerization under dilute conditions using high RAFT/initiator ratios displayed strongly enhanced chromatographic performance in terms of retentivity and enantioselectivity.

Introduction

The engineering of surface confined polymer films has to a large degree benefitted from surface initiated polymerization (SIP) and controlled radical polymerization (CRP) techniques.[1] These films consist of polymer chains of controlled molecular weight tethered with one chain end to the surface. In addition to molecular weight and dispersity control, CRP can be used for quasi-living polymerization to prepare block copolymers of defined architectures to impart various advanced functions. The few reports describing SIP and CRP of crosslinked polymers commonly refer to molecularly imprinted films where a high level of crosslinking is a necessity for preserving the integrity of the imprinted recognition sites.[2–9] In general, the use of grafting techniques for preparing MIP beads allows the bead morphology to be set independently from the formation of the MIP.[10] Hence, materials exhibiting similar bead size and porous properties can be prepared using widely different monomers and solvents. In addition to the above-mentioned structural control, the added value of CRP comes from the degenerative nature of the chain growth leading to shorter, more uniform primary chains and potentially a more regular homogeneous network. The latter may positively impact the fidelity and reduce the binding site heterogeneity commonly observed for molecularly imprinted networks. Indeed, Byrne *et al.* recently demonstrated an enhanced uptake capacity for MIPs prepared by iniferter controlled radical polymerization.[11] Moreover, SIP and CRP are widely employed for synthesising well dispersed multifunctional nanoparticles (*e.g.* for drug delivery, imaging, and diagnostics) and also imprinted nanoparticles[8,12] which can otherwise be difficult to access by alternative approaches such as precipitation polymerization and miniemulsion polymerization.

We recently reported on "grafting from" techniques for the synthesis of MIP composite materials with improved static and dynamic binding properties.[3,10,13] The first of these consisted in the use of immobilized azo-initiators which allowed the synthesis

INFU, Technische Universität Dortmund, Otto-Hahn-Str. 6, 44221 Dortmund, Germany. E-mail: borje@infu.uni-dortmund.de

† Electronic supplementary information (ESI) available. See DOI: 10.1039/c2py00544a

‡ Present address: Max Planck Institute of Colloids and Interfaces, 14424 Potsdam, Germany

View Article Online

Published on 06 February 2012. Downloaded by Michigan State University on 27/01/2016 02:24:16.

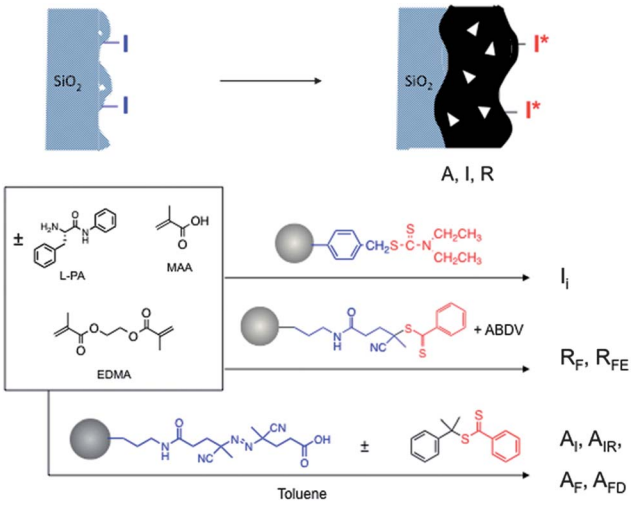

Fig. 1 Grafting of L-phenylalanine anilide (L-PA) imprinted polymer films from a porous silica support modified with azoinitiator (A), iniferter (I) or RAFT agent (R). The grafting was performed using a common prepolymerization mixture to reach low conversions by preinterruption (I subscript) or to reach near full conversions (F subscript) under high dilution (D subscript), using high RAFT/initiator ratio (E subscript) or in the presence of soluble RAFT agent (R subscript).

of thin film MIP composites with much improved mass transfer characteristics (Fig. 1).[10] Some control of the grafting was achieved by the use of immobilized dithiocarbamate initiators (commonly referred to as iniferters) where the mobile radical formed upon decomposition is stable and poor at propagating chains.[3,13] The living character of this polymerization was used for layer by layer grafting of different MIPs onto wide pore silica. A few years ago we investigated the use of soluble chain transfer agents (RAFT agents) as another means of achieving SIP and CRP.[4] The materials could be prepared in a short time and exhibited superior mass transfer properties compared to the traditional imprinted bulk monoliths or materials prepared without the polymerization control through RAFT agents.

Nevertheless several drawbacks of the previously described grafting protocols became obvious. Since the film thickness is controlled by interrupting the polymerization at given times the monomer conversion is low leading to significant batch to batch variations with respect to structure and performance. Moreover unreacted monomer is difficult to recover leading to low overall yields and loss of reagents. The use of light to cleave the immobilized initiator is also problematic since the polymerization is performed in the pore system of solids which cause light scattering and nonuniform intensities.

To address these problems we have recently focused on methods for grafting to reach high monomer conversion and methods relying on thermal homolysis of the initiator. In order to assess the relative merits of interrupted and high conversion grafting techniques for producing homogeneously grafted films, polymers were grafted from a common silica support using an immobilized azo-initiator alone or in the presence of a soluble RAFT agent, an R-immobilized RAFT agent[14] with soluble azo-initiator, or finally by CRP relying on an immobilized iniferter (Fig. 1). Evaluation was performed by characterising the pore structure, morphology and template recognition of the polymers.

Experimental section

Materials

Ethylene glycol dimethacrylate (EDMA), methacrylic acid (MAA), (3-aminopropyl)triethoxysilane (APS) and ethyl chloroformate were obtained from Aldrich (Deisenhofen, Germany). *p*-(Chloromethyl phenyl trimethoxysilane) (CPS) was obtained from Lancaster (Frankfurt am Main, Germany). EDMA was purified by washing consecutively with 10% aqueous NaOH, water, brine and finally with water. After drying over $MgSO_4$, pure, dry EDMA was obtained by distillation under reduced pressure. MAA was purified by distillation under reduced pressure. 4,4′-Azobis(4-cyanopentanoic acid) (ACPA), methanol and acetic acid (AcOH) were obtained from Fluka (Deisenhofen, Germany). Concentrated hydrochloric acid, dichloromethane (DCM), benzene and acetonitrile (ACN) were obtained from Merck (Darmstadt, Germany). The templates L- and D-phenylalanine anilide (L-PA and D-PA) were synthesized following a previously described procedure.[10] Anydrous solvents, dimethyl formamide (DMF), toluene and tetrahydrofuran (THF) were purchased from Fluka and used as received. The following silicas were used as supports. Silica research samples Si-100 supplied by Dr D. Lubda from Merck (Darmstadt) (10 μm average particle size) were used in Table S1†. These were mesoporous with a surface area (S) of 360 $m^2\ g^{-1}$, an average pore diameter (D_p) of 13 nm and a pore volume (V_p) of 1.39 mL g^{-1}. For Si–APS–ACPA the support was Licrosphere Si100 with the following characteristics: $S = 380\ m^2\ g^{-1}$, $D_p = 12$ nm, and $V_p = 1.26$ mL g^{-1}. The soluble RAFT agent (2-phenylprop-2yl-dithiobenzoate) was synthesised according to the method reported by Benicewicz by refluxing benzoic acid and 2-phenyl-2-propanol in the presence of phosphorus pentasulfide in benzene.[15] For the RAFT immobilization (Table S2†) either mesoporous silica beads (Licrosphere Si100) (15 μm average particle size) with a surface area (S) of 320 $m^2\ g^{-1}$ (after treatment with 17% HCl), an average pore diameter (D_p) of 11.6 nm and a pore volume (V_p) of 1.28 mL g^{-1} or macroporous beads (Si500) (Fuji Silysia Japan) (30 μm average particle size) with a surface area (S) of 45 $m^2\ g^{-1}$, an average pore diameter (D_p) of 47.5 nm and a pore volume (V_p) of 0.81 mL g^{-1} were used. The RAFT agent 4-cyanopentanoic acid dithiobenzoate was purchased from Stream Chemicals.

Interrupted grafting of polymer on azo- and iniferter-modified silicas (Table 1)

The grafting was performed in specially designed tubes containing 1 g of azo-modified (series A_I and A_{IR}) or iniferter-modified (series I_I) silica particles (see ESI†) suspended in a polymerisation mixture containing L-PA (0.240 g, 1 mmol), 2-phenylprop-2yl-dithiobenzoate (0.20 g, 0.74 mmol) (series A_{IR}), MAA (0.68 mL, 8 mmol) and EDMA (7.6 mL, 40 mmol) dissolved in 11 mL of dry toluene. After sealing with a rubber septum and mixing, the solutions were purged with N_2 for 15 min. The flasks were then placed in a thermostatted bath set at 15 °C, at 5 cm distance from a high pressure mercury vapour

 This journal is © The Royal Society of Chemistry 2012

View Article Online

Published on 06 February 2012. Downloaded by Michigan State University on 27/01/2016 02:24:16.

lamp (Philips, HPK, 125 W). The subsequent grafting polymerisation was performed for a defined period of time with continuous nitrogen purging. Thereafter, the beads were filtered off, washed with 50 mL of the polymerisation solvent, extracted with methanol in a Soxhlet apparatus for 24 h and dried overnight under vacuum at 40 °C. Non-imprinted control polymer (NIP) composites were prepared as described above but without addition of the template.

Grafting of polymer to near full monomer conversion on azo-modified silica (Table 2)

The grafting was performed in specially designed tubes containing 1 g of azo-modified silica particles suspended in 5 mL (A_F) or 20 mL (A_{FD}) of a mixture containing L-PA (8.0 mg ($d = 1$ nm), 14.0 mg ($d = 2$ nm) or 18.9 mg ($d = 3$ nm)), MAA (23.0 mg ($d = 1$ nm), 41.0 mg ($d = 2$ nm) or 54.1 mg ($d = 3$ nm)) and EDMA (264.5 mg ($d = 1$ nm), 472.2 mg ($d = 2$ nm) or 623.1 mg ($d = 3$ nm)) in dry toluene. These quantities correspond to a molar ratio of L-PA/MAA/EDMA of 1/8/40. After purging the mixture with nitrogen, polymerization was initiated by UV-irradiation at 15 °C for 24 h. After polymerization, the suspended particles were filtered through a sintered glass funnel and extensively washed with methanol/formic acid/water, 80/15/5 (v/v/v) and pure methanol. The composites were finally dried in a vacuum oven at 40 °C for 12 h.

Grafting of polymer to near full monomer conversion on RAFT-modified silica (Table 3)

R_FSi100 series. Si100-RAFT particles (Table S2†) (1 g) were suspended in a prepolymerization mixture containing L-PA (28.9 mg, 0.12 mmol), MAA (0.081 mL, 0.96 mmol) and EDMA (0.905 mL, 4.8 mmol) dissolved in 20 mL of dry toluene. The polymerization mixture was subjected to three freeze–thaw cycles under nitrogen whereafter the initiator ABDV (115 mg (series R_F) and 29 mg (series R_{FE})) was added. This corresponds to a ratio of RAFT/initiator of 0.5 (series R_F) and 2 (series R_{FE}). Polymerization was initiated at 50 °C for 24 h. After polymerization the particles were filtered through a sintered glass funnel and washed with methanol/formic acid/water, 80 : 15 : 5 (v/v/v) and pure methanol and then the polymer was dried under vacuum at 40 °C overnight.

R_FSi500 series. R_F^{500} and R_{FE}^{500} were prepared in a similar manner but the prepolymerization mixture contained L-PA (5.2 mg, 0.022 mmol), MAA (0.015 mL, 0.173 mmol) and EDMA (0.163 mL, 0.865 mmol) and the RAFT/initiator ratio was adjusted to 0.3, 1.4 and 14.

Silica removal

Portions (1 g) of the composite materials were suspended in 10 mL of 3 M NH_4HF_2 (aq.) in Teflon flasks. The suspensions were shaken at room temperature for 2 days and then filtered through a glass funnel. The resulting polymer was washed with water to remove unreacted NH_4HF_2 and dried in a vacuum oven at 40 °C for 24 h.

HPLC measurements and evaluation

The composite materials were typically slurry packed into stainless steel columns (120 × 4 mm or 33 × 4 mm), using MeOH/H_2O 80 : 20 (v/v) as pushing solvent, and evaluated chromatographically. The flow rate was 1 mL min^{-1} or 0.5 mL min^{-1} and 10 μL aliquots of 1 mM solutions of pure enantiomers or racemate were injected unless otherwise mentioned. The elution was monitored at 260 nm. The retention factors (k_L and k_D) and the separation factor (α) were calculated using the following formulae: $k_L = (t_L - t_O)/t_O$; $k_D = (t_D - t_O)/t_O$; $\alpha = k_L/k_D$ where t_L is the retention time of the L-enantiomer, t_D is the retention time of the D-enantiomer and t_O is the retention time of the void marker, acetone.

Results and discussions

The "grafting from" technique for producing L-phenylalanine anilide (L-PA) imprinted composites was investigated using three previously reported initiator systems as depicted in Fig. 1. The first relies on silica immobilized iniferters (I) where initiation starts by a reversible photoinduced cleavage of a C–S bond to result in an active carbon centered radical capable of initiating chains and a stable dithiocarbamate centered radical.[16] The second system (A) is based on conventional azoinitiators immobilized onto silica decomposable by either thermolysis or photolysis,[17] whereas the third (R) relies on chain transfer agents (RAFT) immobilized onto the silica surface *via* the R-group[14] (Tables S1 and S2†) where surface grafting requires a source of primary radicals generated in the solution phase. In order to compare the relative merits of these techniques we grafted imprinted copolymers of methacrylic acid and ethylene glycol dimethacrylate under similar conditions following the protocols outlined in Fig. 1 *i.e.* in a 1 : 5 molar ratio in the presence of 5 mol% L-phenylalanine anilide as chiral template and toluene as solvent. The common support was mesoporous silica (Si100) with a high surface area ($S = 380$ m^2 g^{-1}) allowing support modifications to be conveniently monitored by conventional techniques *e.g.* IR spectroscopy, elemental analysis, gravimetric techniques and nitrogen sorption analysis. The use of a chiral template allowed achiral non-specific binding to be easily deconvoluted from enantioselective binding caused by imprinting.

Synthesis and characterisation of initiator or RAFT modified supports

Azoinitiator and iniferter modified silicas were synthesised according to previously reported methods. As shown in Table S1† this resulted in a surface coverage of initiators in accordance with our previous investigations. This value was 6.4% of the available sites for the iniferter modified silica (SiDTC) whereas the azoinitiator modified silicas (SiACPA) exhibited surface coverages of 2.5% (a) and 18% (b). Although the initiator surface coverage was not fully optimized low coverages were preferred in order to minimize early recombinant termination (ligand–ligand distance > 1 nm) and, for non-controlled polymerizations, to delay the bulk macrogelation. However, for the RAFT controlled polymerizations, a higher coverage could still be tolerated. The RAFT modified supports (Si100-RAFT and Si500-RAFT) were synthesised by ethyl chloroformate catalyzed

View Article Online

Published on 06 February 2012. Downloaded by Michigan State University on 27/01/2016 02:24:16.

coupling of 4-cyanopentanoic acid dithiobenzoate to amino-modified silica to reach a final coverage of 7.6% for the Si100 support and 27% for the Si500 support (Table S2†).

Composites prepared by interrupted grafting

Synthesis and characterisation. Prior to polymerization the modified silica particles were suspended in the prepolymerization mixtures shown in Fig. 1. Batches of 1 g were suspended in *ca.* 20 mL prepolymerization mixture in test tubes sealed with rubber septa. The latter were immersed in a thermostatted water bath and placed symmetrically around a UV light source under continuous purging and agitation with nitrogen. The polymerization was thereafter initiated by UV light using a 125W mercury medium pressure lamp with an emission spectrum overlapping the absorption bands of the initiators. Samples were withdrawn at regular time intervals and the resulting composite particles subjected to extensive extraction with methanol in a Soxhlet apparatus, dried and subsequently investigated for the density of grafted polymer. Due to the high surface area of the silica beads, several alternative techniques can be used herefore, *i.e.* infrared spectroscopy (monitoring the normalized C=O stretch at 1700 cm^{-1}), gravimetry or thermal gravimetric analysis (TGA), nitrogen sorption (average pore size distribution) and elemental analysis.[10] For homogeneously grafted films, estimates of film thickness based on the three latter techniques display good agreement whereas estimates based on the nitrogen sorption isotherm for heterogeneously grafted films are likely to disagree with the other values.

Table 1 shows the time course of grafting based on the carbon content for the three different series. The amount of grafted polymer increases continuously with time as reflected in the increase in carbon content, mass and the changing pore dependent parameters.

For perfectly living polymerizations the immobilized dithiocarbamate groups of the iniferter (series I_I) and the dithioesters of the RAFT agent (series A_{IR}) should be quantitatively found as end groups of the grafted polymer films. The low sulfur contents indicate that this is not the case. Thus the sulfur contents of the iniferter grafted composites are *ca.* 30% lower than the ideal value whereas for the RAFT mediated grafting the values are *ca.* 50% lower. One explanation for this deviation is that chains are being irreversibly terminated by chain recombination. This is particularly likely for surface confined radicals propagating with similar rates.[14] However, we previously showed that iniferter based grafting on wide pore silica exhibited living properties since multiple layers could be grafted consecutively on one support.[3] TGA supported the elemental analysis results although in general this technique gave somewhat higher graft densities. Thus mass loss curves typical for monolithic polymers were obtained with a 50% of the total mass loss occurring at *ca.* 325 °C for an I_I composite and 389 °C for an A_{FD} composite (Fig. 2).

Nitrogen sorption isotherms are informative of the homogeneity of the grafted polymer films (*vide supra*). The isotherms for all the composites were of type IV exhibiting a hysteresis profile which indicates mesoporosity (see Fig. 3). A closer inspection however reveals pronounced differences between the iniferter based composites (I_I) and the azoinitiator based counterparts (A_I). Thus, whereas the latter exhibit a continuous drop in the volume at atmospheric pressure and closed hysteresis loop, the

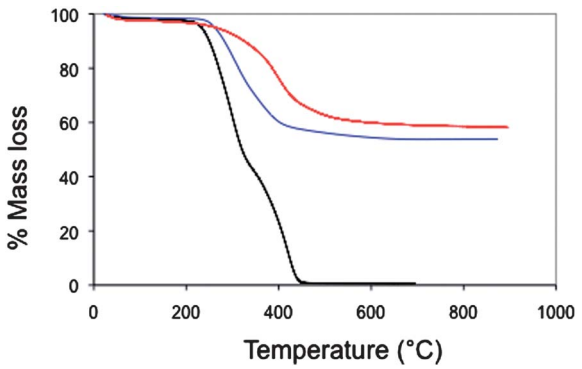

Fig. 2 TGA mass loss curves obtained for A_{FD}^{2} (red curve), I_I^{360} (blue curve) and P_{ref} (black curve). See Tables 1 and 2 for polymer assignments.

Table 1 Characteristics of molecularly imprinted polymer composites prepared by interrupted photoinitiated grafting from silica modified with iniferter or azoinitiator in the presence or absence of a RAFT agent

Composite[a]	Polym. time/min	%C	%N	%S	Δm/g g^{-1}	d [b]/nm	S [c]/m^2 g^{-1}	D_p [c]/nm	V_p [c]/mL g^{-1}
A_{IR}^{60}	60	15.6	4.40	0.32	0.35	0.9	192	11.5	0.66
A_{IR}^{90}	90	17.4	4.43	0.31	0.42	1.1	192	11.5	0.69
A_{IR}^{120}	120	18.7	4.56	0.29	0.51	1.2	193	11.4	0.65
A_{IR}^{240}	240	19.9	4.83	0.30	0.58	1.4	181	9.9	0.59
A_I^{60}	60	16.0	2.43	—	0.39	1.0	285	10.6	0.70
A_I^{90}	90	21.0	2.25	—	0.52	1.5	280	10.2	0.63
A_I^{120}	120	23.0	2.37	—	0.97	1.7	265	9.0	0.60
I_I^{60}	60	16.6	0.14	0.70	0.58	1.0	209	7.1	0.64
I_I^{120}	120	17.2	0.15	0.69	0.64	1.1	142	3.8	0.14
I_I^{240}	240	20.0	0.16	0.75	0.72	1.4	257	3.9	0.30
I_I^{360}	360	23.4	0.15	0.77	0.97	1.8	197	3.7	0.36
P_{ref}	24 h	58	0.23	—	—	—	358	23.02	0.68

[a] The composites were prepared by interrupted photoinitiated grafting of imprinted polymers for the indicated times from silica modified with iniferter (I_I) or azoinitiator in the presence (A_{IR}) or absence (A_I) of a RAFT agent following the methods described in the Experimental section using Si-ACPA[a] (A_I-composites), Si-ACPA[b] (A_{IR}-composites) or Si-DTC (I-composites) as supports. Data for a corresponding reference polymer P_{ref} prepared following conventional solution polymerization have been added. [b] The film thickness estimated from the carbon content of the grafted film. [c] The BET specific surface area (S), specific pore volume (V_p) and average pore diameter (D_p) were calculated from the nitrogen adsorption isotherms as described in the Supporting Information.

 This journal is © The Royal Society of Chemistry 2012

View Article Online

Published on 06 February 2012. Downloaded by Michigan State University on 27/01/2016 02:24:16.

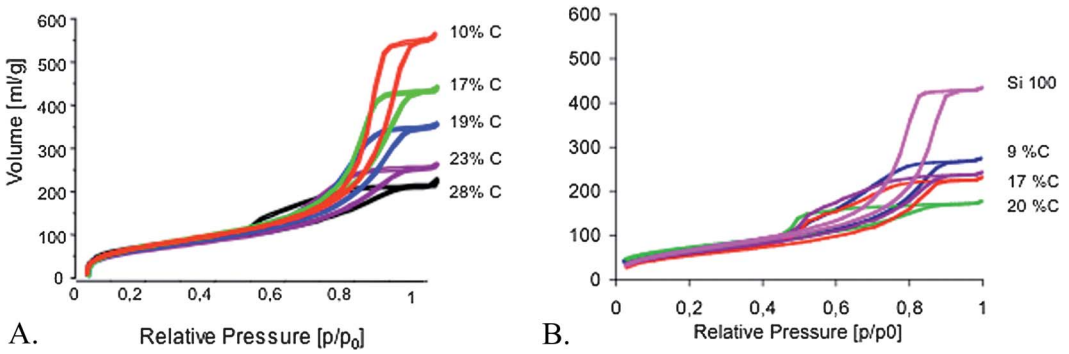

Fig. 3 Nitrogen sorption isotherms of the A_I composites (A) and I_I composites (B) containing different densities (%C) of grafted polymer.

latter isotherms exhibit a discontinuous drop and a desorption branch which often do not close with the adsorption branch. This is indicative of volume changes in the material upon pore filling with nitrogen.

The desorption branch was used to calculate the pore size distribution of the composites (Fig. 4). From these it can be concluded that the azoinitiator based composites exhibit pore size distributions similar to the original silica support with a maximum near 10 nm.

This contrasts with the graphs for the iniferter based composites showing a much lower average pore diameter with two maxima, a broad near 6 nm and a narrow presumably an artifact near 4 nm. The former decreased whereas the latter increased with increasing grafting density. The different quality of the composites is perhaps best illustrated by the plots showing the pore system parameters plotted *versus* the carbon content of the materials (Fig. 5).

Here the azoinitiator based composites exhibit linearly decreasing values with %C whereas the iniferter based composites exhibit a drop at low %C whereafter the values change only little at higher carbon contents. These results show clearly that the photoinduced iniferter grafting from mesoporous supports does not produce homogeneously grafted films under the present conditions. This disagrees with our previous report and others where the average pore size indeed decreased continuously with the grafting content. A possible reason for this contradiction may

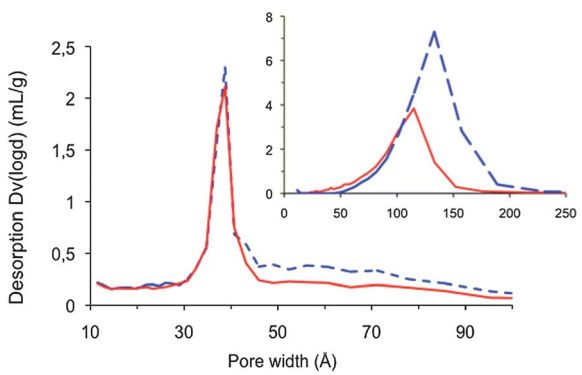

Fig. 4 Pore size distribution of I_I^{240} (blue dashed line) and I_I^{360} (red solid line) calculated from the desorption branch of the isotherm obtained from nitrogen sorption measurements. The inset shows the pore size distribution of the bare silica support (dashed line) and A_{IR}^{90} (solid line).

be the different supports that were used (a wide pore silica was used in our previous study (D_p = 100 nm)) which could have caused a better refractive index match between the silica support and the pore filling solution. This source for the heterogeneity appears to be more important for the iniferter based composites. Indeed, TEM images of cross-sections of the iniferter composites featured an apparently denser particle periphery compared to bare silica and to the azo-based composites (Fig. 6).

This contrasts with the results of a more detailed TEM analysis of macroporous grafts which were concluded to homogeneously cover the interior of the particles.[18]

As expected from the linear dependence of D_p *versus* %C for the A_I series (Fig. 5A), the average film thickness calculated based on these two parameters exhibited a linear correlation (Fig. 7).

The slightly larger than unity slope is likely due to an overestimate of the film density (D = 1) which in turn leads to an underestimation of d calculated based on %C. The quality of the grafted films can also be investigated for their ability to protect the underlying support from etching reagents. Hence, we exposed the composites to a fluoride solution and measured the loss of silica at given time intervals (Table S3†). The results showed that all silica was quantitatively removed from the iniferter-grafted composite after two days of etching whereas the azo-grafted composite required an additional five days of soaking in the fluoride solution to fully lose the silica support.

In agreement with the TEM image in Fig. 6, SEM images of the polymers remaining after fluoride etching of the iniferter composite revealed a relatively smooth surface texture with small pores whereas the corresponding azo-material displayed both meso- and macro-pores (Fig. S1†). Collectively these results demonstrate that the azo-grafted films are homogeneously covering the support whereas the iniferter-grafted films are heterogeneous with abundant defects.

In order to better understand the structure of the grafted films they were further characterised by spectroscopy (IR and NMR). Whereas the IR spectra showed no significant differences in the spectral features (Fig. S2†). ^{13}C-CP-MAS solid state NMR spectra revealed differences in the relative signal intensities of the different nuclei (Fig. S3†). Signals corresponding to the iniferter group are clearly visible indicating its successful incorporation. More interesting are the different signal intensities corresponding to the pendent unreacted double bonds at 168 ppm. When normalized to the intensity of the CO signal, this signal is

View Article Online

Published on 06 February 2012. Downloaded by Michigan State University on 27/01/2016 02:24:16.

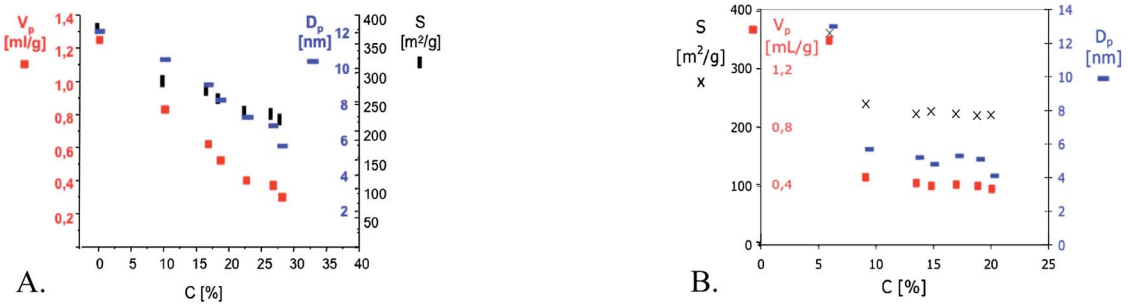

Fig. 5 Total pore volume (V_p) (red squares), average pore diameter (D_p) (blue horizontal lines) and surface area (S) (black vertical lines (A) or crosses (B)) derived from nitrogen sorption isotherms *versus* the carbon content of the composite particles A_I (A) and I_I (B).

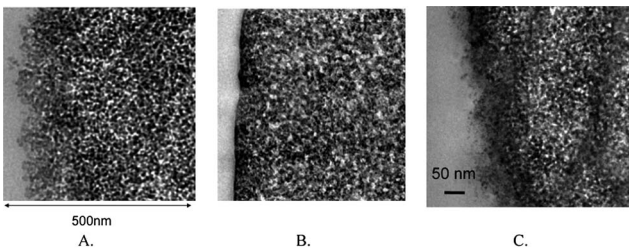

Fig. 6 Transmission electron micrographs of (A) the bare silica support Si100, (B) imprinted I_I^{120} and (C) A_F^3. At locations containing silica the image appears black or darker due to the larger electron scattering cross-section of the locations containing heavier elements.

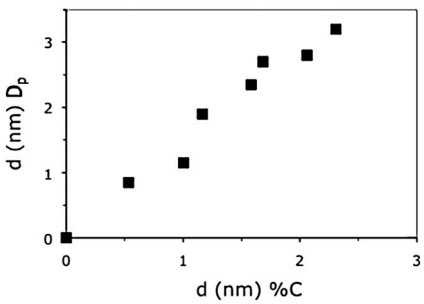

Fig. 7 Average thickness (d) of the grafted polymer films of the A_I composites estimated from the average pore diameter (D_p) *versus* an estimate of the same based on the carbon content of the composites.

significantly weaker in the composites generated from the iniferter system compared to the azo-based composites. This indicates a higher conversion of pendent double bonds and agrees with the observation made by Hutchison *et al.* based on their studies of iniferter initiated polymerizations of multifunctional monomers.[19]

Chromatographic evaluation. Chromatographic tests reveal whether the template has been successfully imprinted as well as the quality, heterogeneity and accessibility of corresponding imprinted sites.[20] As seen in Fig. 8, the elution profiles resulting from the injection of racemates or separate enantiomers corresponding to the template (L-phenylalanine anilide, LPA) appeared very different depending on which stationary phase was used. The iniferter based composites (I_I^{240}) exhibited low enantioselectivities and were never capable of resolving the

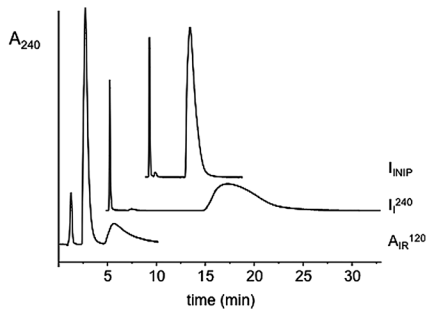

Fig. 8 Elution profiles of DL-PA injected (10 μL of a 1 mM solution) as a racemate (A_{IR}^{120}) or separately (I_I) into columns (120 × 4.5 mm) packed with the indicated L-PA imprinted composites. Mobile phase: A_{IR}^{120}: MeCN/sodium acetate buffer, 0.01 M, pH 4.8: 70/30 (v/v); I_I: MeCN/H_2O/HOAc: 92.5/5/2.5 (v/v/v).

racemates. Nevertheless, a strongly enhanced retention was observed compared to a non-imprinted composite (I_{INIP}). Another problem with these phases was a slight drift in the retention factors observed with time. This behaviour may be related to the inferior homogeneity of these grafted films (see the previous section) and the swelling effects mentioned in the context of the nitrogen sorption isotherms.

As expected, the best performance was obtained using the azoinitator based composites (A_I and A_{IR}). In this case, the resolution of the racemates was observed when the thickness of the grafted film exceeded the critical value of *ca.* 1 nm, leading to complete base line resolutions at higher grafting densities (as for A_{IR}^{120} in Fig. 8).

Additional strong evidence for the presence of a homogeneously grafted film came from a comparison of two composites prepared from the same prepolymerization mixture with identical carbon contents of 11% (Fig. 9).

The only difference between these materials was the support morphology, one being the mesoporous Si100 support with an average surface area of 380 $m^2\ g^{-1}$ and the other an Si1000 material[10] with an area of 33 $m^2\ g^{-1}$. Interestingly, in spite of the identical composition only the material prepared using the wide pore silica exhibited enantioselectivity and was capable of resolving the racemate. This can be explained considering the average apparent film thickness for composites with a carbon content of 11%. Thus for the mesoporous support the thickness would be less than 1 nm whereas for the wide pore support it would be *ca.* 6 nm. Obviously, considering the template size

 This journal is © The Royal Society of Chemistry 2012

View Article Online

Published on 06 February 2012. Downloaded by Michigan State University on 27/01/2016 02:24:16.

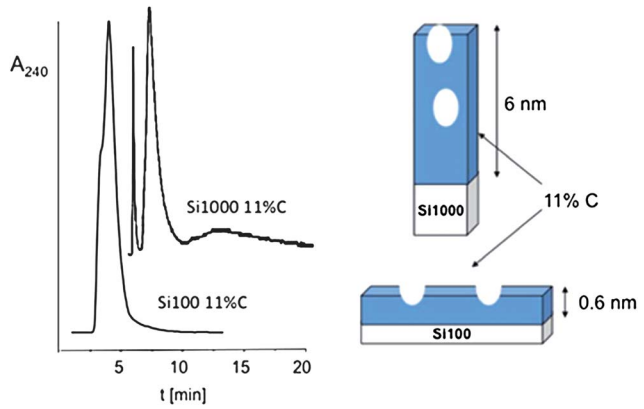

Fig. 9 Elution profiles of DL-PA injected (10 μL of a 1 mM solution) into columns (33 × 4 mm) packed with L-PA imprinted composites with identical graft densities (11 %C) prepared by azoinitiated interrupted grafting using a low surface area support (Si1000: 33 m^2 g^{-1}) (upper profile) and a high surface area support (Si100: 380 m^2 g^{-1}) (lower profile). The average film thickness (*d*) indicated in the cartoon on the right was estimated from the carbon content assuming a homogeneous liquid film with a unit density.

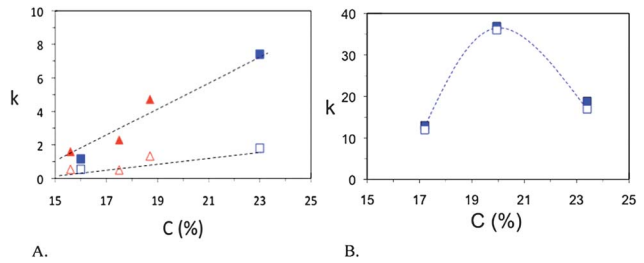

Fig. 10 Plot of retention factors (*k*) for L-PA (solid symbols) and D-PA (open symbols) *versus* carbon content (%C) for (A) the A_I (blue squares) and A_{IR} (red triangles) series composites and in (B) the I_I series composites. Mobile phase: MeCN/H_2O/HOAc: 92.5/5/2.5 (v/v/v).

(roughly 13 Å end to end distance) the former films are too thin to host shape complementary sites with converging functional groups. This would not be the case for the films grafted on the wide pore silica which would be thick enough to host such sites.

Plotting the chromatographic retentivity and enantioselectivity *versus* the amount of grafted polymer is another way to study the quality and homogeneity of the grafted films.[10] Again the shapes of the curves are completely different for the iniferter and the azo-based composites. Whereas the azo-composites, prepared both in the presence and absence of a soluble RAFT agent, feature an apparent linear increase in the template (L-PA) retention factor and enantioselectivity with increasing graft density (Fig. 10), the plot for the iniferter composites features a maximum retentivity at an intermediate graft density whereafter retention drops. The latter would be a reasonable consequence of the presence of a denser shell which for higher graft densities will become less and less permeable.

Composites prepared by grafting to high conversion

Due to the aforementioned limitations of the kinetically controlled grafting (poor reproducibility, low overall yields, non-stoichiometric monomer incorporation, and film heterogeneity) grafting protocols relying on quantitative monomer conversions are expected to offer general improvements. An obvious approach is here to simply adjust the addition of monomer assuming it to be fully incorporated in the grafted film. A theoretical film thickness can then be calculated under the assumption that the added monomer will form a liquid film covering the entire surface of the support. We therefore adjusted the total monomer addition to correspond to films with 1, 2 and 3 nm average thickness followed by photoiniated grafting at two different dilutions with an inert solvent. As seen in Table 2 all parameters indicated successful formation of grafted films with an average thickness and density roughly proportional to the quantity of added monomer. Hence, the carbon content, although generally higher than for the composites prepared by interrupted polymerization, increased whereas the nitrogen content, given the lack of nitrogen in the grafted film, showed a decrease with added monomer. The composites prepared under high dilution displayed somewhat lower graft densities and higher pore volumes but were similar with respect to the transmission FTIR spectra in Fig. S4†.

The dilution did however strongly influence the chromatographic properties of the composites. Fig. 11 shows the retention factor *versus* graft density for the composites reported in Table 2. Composites prepared from concentrated monomer solution feature much lower retention factors and enantioselectivities compared to the composites prepared in the dilute

Table 2 Characteristics of molecularly imprinted polymer composites prepared by photoinitiated grafting to high monomer conversion from silica modified with azoinitiator

Composite[a]	%C	%N	Mass loss (%)	*d* [b]/nm	*S* [c]/m^2 g^{-1}	D_p[c]/nm	V_p[c]/mL g^{-1}	Conversion[d] (%)
A_F^1	22.8	2.40	37	2.1	335	4.1	0.45	82
A_F^2	28.2	2.10	44	3.0	125	3.5	0.17	72
A_F^3	31.0	1.72	51	3.7	129	3.7	0.14	75
A_{FD}^1	20.6	2.52	33	1.8	243	4.1	0.40	64
A_{FD}^2	24.6	2.33	40	2.4	174	4.1	0.27	57
A_{FD}^3	26.5	1.98	46	2.7	214	3.7	0.25	60

[a] The composites were prepared by photoinitiated grafting to high monomer conversion from silica modified with azoinitiator Si-ACPA[a] in a non-diluted (5 mL) (A_F) or diluted (20 mL) (A_{FD}) system to 1, 2 or 3 nm film thickness. [b] The film thickness estimated from the carbon content of the grafted film. [c] The BET specific surface area (*S*), specific pore volume (V_p) and average pore diameter (D_p) were calculated from the nitrogen adsorption isotherms as described in the Supporting Information. [d] Monomers converted into grafted polymer (%) calculated based on thermogravimetry assuming a contribution to the mass loss of 17% from the initiator modified silica Si-ACPA[a].

View Article Online

Published on 06 February 2012. Downloaded by Michigan State University on 27/01/2016 02:24:16.

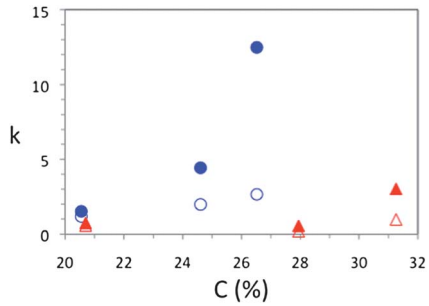

Fig. 11 Plot of retention factors (k) for L-PA (solid symbols) and D-PA (open symbols) *versus* carbon content (%C) for A_{FD} (blue circles) and the A_F (red triangles) series composites. Mobile phase: MeCN/acetate buffer pH 4.8: 70/30 (v/v).

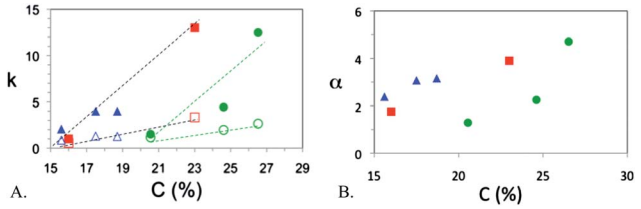

Fig. 12 (A) Plot of retention factors (k) for L-PA (solid symbols) and D-PA (open symbols) *versus* carbon content (%C) for the A_I (red squares), A_{IR} (blue triangles) and A_{FD} (green circles) series composites. In (B) the corresponding separation factor (α) is plotted. Mobile phase: MeCN/acetate buffer pH 4.8: 70/30 (v/v).

system, in spite of the higher carbon content of the former. Interestingly the retentivity and selectivity of the A_{FD} series are comparable to those of the A_I series (Fig. 12). Hence in the same mobile phase, the A_I series feature an increase in k_L *versus* %C with a slope that is similar to that of the A_{FD} series, the difference being that the latter carbon contents are overall higher. Plotting the same values against the IR normalized band intensity (see Fig. S6†) of the carbonyl stretch at 1700 cm^{-1} led to a graph where the two curves had switched place *i.e.* where k increased at lower intensities on A_{FD} than on A_I. This implies that the excessive carbon content originates from the underlying support. This also shows that the quality of these grafted films in terms of imprinting is rather similar—a surprising finding in view of the different techniques used in their preparation.

The final problems we decided to address are related to the use of immobilized azoinitiators. These solids are poorly stable, require cold storage and are therefore impractical to handle. Moreover attempts to use these for thermally initiated polymerizations have failed. In order to enhance the method robustness from this aspect we therefore decided to immobilize a RAFT CTA. Direct condensation of 4-cyanopentanoic acid dithiobenzoate with surface amino groups led to a RAFT modified support with the RAFT agent immobilized *via* its R group (Fig. 1).[14] Addition of a propagating radical to the dithioester will here generate a tertiary carbon-centered radical identical to the one resulting from photolysis of the azo-modified

Table 3 Characteristics of molecularly imprinted polymer composites prepared by thermally initiated grafting to high monomer conversion from silica modified with a RAFT agent

Composite[a]	Support	RAFT/ABDV	%C	%N	Mass loss (%)	S [b]/m^2 g^{-1}	D_p [b]/nm	V_p [b]/mL g^{-1}	Conversion[c] (%)
R_F^{Si100}	Si100-RAFT	0.5	32.1	0.85	56	207	4.1	0.25	70
R_{FE}^{Si100}	Si100-RAFT	2.0	31.7	0.81	56	260	3.7	0.33	70
R_F^{Si500}	Si500-RAFT	0.3	11.0	0.72	17	68	32	0.39	60
R_{FE}^{Si500}	Si500-RAFT	1.4	10.6	0.74	19	72	32	0.35	73
R_{FE2}^{Si500}	Si500-RAFT	14	12.7	0.99	20	57	24	0.31	74

[a] The composites were prepared by thermally initiated grafting to high monomer conversion from different silica supports modified with a RAFT agent using different ratios of RAFT agent to azoinitiator (ABDV). [b] The BET specific surface area (S), specific pore volume (V_p) and average pore diameter (D_p) were calculated from the nitrogen adsorption isotherms as described in the Supporting Information. [c] Monomers converted into grafted polymer (%) calculated based on thermogravimetry assuming a contribution to the mass loss from the initiator modified silicas as specified in Table S2†.

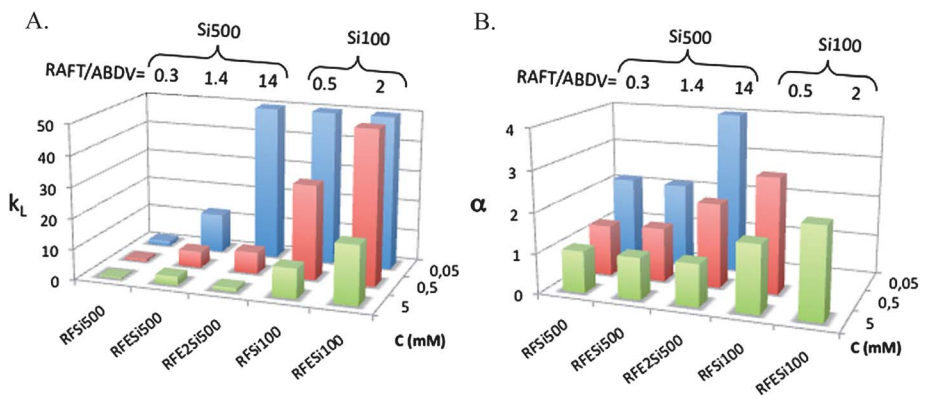

Fig. 13 Plot of retention factors (k) for L-PA (A) and associated separation factors (α) (B) at three different sample loads for L-PA imprinted composites prepared by grafting from different RAFT modified supports. The RAFT/ABDV ratio and type of silica support have been indicated above the graphs. Mobile phase: MeCN.

 This journal is © The Royal Society of Chemistry 2012

View Article Online

Published on 06 February 2012. Downloaded by Michigan State University on 27/01/2016 02:24:16.

silica. Hence external addition of a soluble initiator is here required. Adjusting the quantity of soluble initiator in relation to the immobilized RAFT agent offers here a simple means of controlling the kinetics of the grafting.

Grafting was therefore performed from a dilute prepolymerization mixture (*vide supra*), tuned to generate thicker films with 3–4 nm average thickness, in the presence of different amounts of ABDV corresponding to the molar ratios of RAFT/ABDV given in Table 3. The presence of the RAFT dithioester groups post-grafting was indicated by the characteristic pinkish color (Fig. S7†) which was of similar intensity as prior to grafting.

In view of the similar graft conversions (Table 3), the reaction appears to have run to similar overall conversions, also for the elevated RAFT/ABDV ratios where propagation is expected to be significantly slower. It was then striking to observe the pronounced influence this parameter had on the retentivity and enantioselectivity of the composites (Fig. 13). With increasing RAFT/ABDV a strong increase in both retentivity and enantioselectivity was observed for both the mesoporous (Si100) and macroporous (Si500) supports. Obviously the RAFT control has here a positive influence on the quality of the imprinted films.

Conclusions

In this study we have critically appraised different techniques to graft imprinted polymers with respect to the robustness, synthetic accessibility, versatility and composite performance. The interrupted polymerization technique suffers from several drawbacks but foremost are those related to batch to batch reproducibility and low yield. The degree of monomer conversion into grafted films was less than 12% for the composites reported in Table 1. Also, the two methods that we applied resulted in films of different qualities. The iniferter based grafting produced heterogeneous composites whereas the azografting produced homogeneous films covering the entire inner pore wall surface. These morphologies influence the chromatographic molecular recognition and mass transfer properties of the materials after imprinting. In both respects, the azobased grafting is superior over the iniferter counterpart leading to high surface area beads with high enantioselectivity. The failure of the former technique can have many origins. Iniferters decompose uniquely by photolysis under absorption of UV light in the region 260–290 nm and a weaker absorption at 340 nm.[21] Azobased initiators can on the other hand decompose thermally or photochemically, the latter at a wavelength of *ca.* 340 nm. Whereas the former decompose to one mobile stable free radical and one surface confined propagating radical immobilized azoinitiator decomposes to two active radicals, thus propagation occurs in solution as well as on the surface. Adding a chain transfer agent in the latter case leads to a reduced rate of propagation and less termination by recombination which may, as for iniferter polymerizations, result in a more homogeneous network with a higher overall monomer conversion.[11] However, this offer no explanation for the poor enantioselectivity displayed by these materials. Instead, as indicated from the SEM and TEM micrographs (Fig. 6 and S1†) the beads exhibit a higher density of polymer near their periphery and a more open structure in their interiors. The reason for this heterogeneity may be a poor refractive index match and/or an initiator decomposition rate that is too fast. Due to the slower mass transfer inside the beads, the latter would result in chain growth mainly at the particle periphery, where mass transfer is not a problem. This would effectively close off the interior of the beads or at least reduce the access to it. Still, these beads do exhibit imprinting effects but to a much lesser extent than the azobased systems. The latter showed a pronounced influence of film thickness on imprintability *i.e.* a minimum thickness of 1 nm was required to produce any detectable discrimination between the two enantiomers. Considering the size of the template L-PA with a 1.3 nm end to end distance in the minimum energy conformation it is reasonable that the polymer matrix would have to protrude at least this distance to offer enantiodiscriminative sites relying on convergent interactions in 3D. This also corroborates our finding that the azo-based grafts exhibit a much more even coverage of the surface.

Significant improvements were achieved by allowing the grafting to proceed to high conversions and by introducing immobilized RAFT agents. The latter offers a fully reproducible procedure for grafting which can be applied to both photo- and thermal initiator homolysis and to different monomers and solvents ranging from non-aqueous styrene/divinylbenzene to aqueous acrylamide based systems. Particularly interesting was the pronounced effect of monomer dilution and the RAFT/initiator ratio on the quality of the imprinted films, in terms of chromatographic retentivity and enantioselectivity (Fig. 11–13). How can these effects be rationally explained? A low dilution corresponds to a high monomer and subsequent radical concentration, an increased rate of propagation, and potential film inhomogeneities due to diffusion limited reactions. This may also cause unwanted macrogelation. At higher dilutions on the other hand the rate of propagation will be slower but this will in turn give the monomers more time to diffuse into the pore system of the beads. The quality of the resulting films is likely to be higher. Counteracting this effect is the dilution effect on the monomer–template complex stability. A more dilute system will promote dissociation of the complex but given that the solvent promotes complex formation this effect may become less important. In this particular case the favorable factors seem to outweigh the latter.

The effect of the RAFT/initiator ratio can be explained in similar terms. Referring to the previous report by Byrne *et al.* one can expect that an increase in the RAFT/initiator ratio will lead to a decrease in the average kinetic chain length and the dispersity of those chains.[11] This can be envisaged to result in a more homogeneous distribution of crosslinks which combined with the slower propagation *per se* will in turn increase the accessibility and possibly produce a more uniform distribution of imprinted sites. This effect has previously been observed for imprinted amorphous network polymers but has not been demonstrated for grafted systems. As for the dilution effects discussed above, the slower propagation will also here result in a more evenly grafted film covering the entire inner surface of the particles.

View Article Online

Acknowledgements

The authors wish to acknowledge the financial support from the European Commission under FP7—Marie Cure Actions, contract PITN-GA-2008-214226 [NEMOPUR] and from the Deutsche Forschungsgemeinschaft DFG (Se777/5-2).

References

1 R. Barbey, L. Lavanant, D. Paripovic, N. Schuwer, C. Sugnaux, S. Tugulu and H.-A. Klok, *Chem. Rev.*, 2009, **109**, 5437–5527.
2 H. Y. Wang, T. Kobayashi and N. Fujii, *J. Chem. Technol. Biotechnol.*, 1997, **70**, 355–362.
3 B. Sellergren, B. Rückert and A. J. Hall, *Adv. Mater.*, 2002, **14**(17), 1204–1208.
4 M.-M. Titirici and B. Sellergren, *Chem. Mater.*, 2006, **18**, 1773–1779.
5 H.-J. Wang, W.-H. Zhou, X.-F. Yin, Z.-X. Zhuang, H.-H. Yang and X.-R. Wang, *J. Am. Chem. Soc.*, 2006, **128**, 15954–15955.
6 X. Wei and S. M. Husson, *Ind. Eng. Chem. Res.*, 2007, **46**, 2117–2124.
7 C.-H. Lu, W.-H. Zhou, B. Han, H.-H. Yang, X. Chen and X.-R. Wang, *Anal. Chem.*, 2007, **79**, 5457–5461.
8 N. Perez-Moral and A. G. Mayes, *Macromol. Rapid Commun.*, 2007, **28**, 2170–2175.
9 F. G. Tamayo, M. M. Titirici, A. Martin-Esteban and B. Sellergren, *Anal. Chim. Acta*, 2005, **542**, 38–46.
10 C. Sulitzky, B. Rückert, A. J. Hall, F. Lanza, K. Unger and B. Sellergren, *Macromolecules*, 2002, **35**, 79–91.
11 A. D. Vaughan, S. P. Sizemore and M. E. Byrne, *Polymer*, 2007, **48**, 74–81.
12 Y. Peng, Y. Xie, J. Luo, L. Nie, Y. Chen, L. Chen, S. Du and Z. Zhang, *Anal. Chim. Acta*, 2010, **674**, 190–200.
13 B. Rückert, A. J. Hall and B. Sellergren, *J. Mater. Chem.*, 2002, **12**, 2275–2280.
14 C. Li, J. Han, C. Y. Ryu and B. C. Benicewicz, *Macromolecules*, 2006, **39**, 3175–3183.
15 A. Sudalai, S. Kanagasabapathy and B. C. Benicewicz, *Org. Lett.*, 2000, **2**, 3213–3216.
16 T. Otsu and M. Yoshida, *Makromol. Chem. Rapid Commun.*, 1982, **3**, 127.
17 O. Prucker and J. Rühe, *Macromolecules*, 1998, **31**, 602–613.
18 B. Rückert and U. Kolb, *Micron*, 2005, **36**, 247–260.
19 J. B. Hutchison, A. S. Lindquist and K. S. Anseth, *Macromolecules*, 2004, **37**, 3823–3831.
20 The degree of template removal from this type of networks has been found to exceed 90% indicating a high level of accessible binding sites. See A. Ellwanger, L. Karlsson, P. K. Owens, C. Berggren, C. Crecenzi, K. Ensing, S. Bayoudh, P. Cormack, D. Sherrington and B. Sellergren, *Analyst*, 2001, **126**, 784–792.
21 Y. Nakayama and T. Matsuda, *Langmuir*, 1999, **15**, 5560–5566.

Published on 06 February 2012. Downloaded by Michigan State University on 27/01/2016 02:24:16.

 This journal is © The Royal Society of Chemistry 2012